



**HAL**  
open science

# Remote Sensing of Mountain Permafrost Landscape by Multi-Fusion Data Modeling. Example of Verkhoyansk Ridge (Russia)

Sébastien Gadal, Moisei Ivanovich Zakharov, Yuri Danilov, Jūratė Kamičaitytė

## ► To cite this version:

Sébastien Gadal, Moisei Ivanovich Zakharov, Yuri Danilov, Jūratė Kamičaitytė. Remote Sensing of Mountain Permafrost Landscape by Multi-Fusion Data Modeling. Example of Verkhoyansk Ridge (Russia). IGARSS 2020, IEEE International Geoscience and Remote Sensing Symposium, Sep 2020, Online, United States. pp.3082-3085. hal-02951488

**HAL Id: hal-02951488**

**<https://hal.science/hal-02951488>**

Submitted on 1 Oct 2020

**HAL** is a multi-disciplinary open access archive for the deposit and dissemination of scientific research documents, whether they are published or not. The documents may come from teaching and research institutions in France or abroad, or from public or private research centers.

L'archive ouverte pluridisciplinaire **HAL**, est destinée au dépôt et à la diffusion de documents scientifiques de niveau recherche, publiés ou non, émanant des établissements d'enseignement et de recherche français ou étrangers, des laboratoires publics ou privés.

# REMOTE SENSING OF MOUNTAIN PERMAFROST LANDSCAPE BY MULTI-FUSION DATA MODELING. EXAMPLE OF VERKHUYANSK RIDGE (RUSSIA)

*Sébastien Gadal*<sup>1,2</sup> *Moisei Zakharov*<sup>1,2</sup> *Yuri Danilov*<sup>2</sup> *Jūratė Kamičaitytė*<sup>3</sup>

<sup>1</sup> Aix-Marseille Univ, CNRS, ESPACE UMR 7300, Univ Nice Sophia Antipolis, Avignon Univ, 13545 Aix-en-Provence.

<sup>2</sup> North-Eastern Federal University, 670000 Yakutsk, Republic of Sakha, Russian Federation.

<sup>3</sup> Kaunas University of Technology, Kaunas, Lithuania.

## ABSTRACT

Mapping of permafrost mountain landscape of Verkhoyansk in the Arctic zone is based on the recognition by remote sensing and GIS modeling of the landscape permafrost-objects resulting from the combination of the Milkov's taxonomic classifications. The methodology developed integrates three types of modeling: the first one is mapping the vegetation repartition using Sentinel 2A with SVM classifier during the summer vegetative period; second is the landform classification using Jenness's algorithm from ASTER data; and the third one is land surface temperature calculus from Landsat 8 OLI/TIRS images identifying the permafrost characteristics categories. Results are merged using a native index equation of permafrost landscape objects in GIS. This original mapping approach improves significantly the understanding of complexity of the permafrost mountain structures and processes with the annual monitoring by remote sensing.

**Index Terms**— Multi-fusion methods, land surface temperature, landform classification, permafrost landscape mapping

## 1. INTRODUCTION

Arctic permafrost mountain landscape is a combination of five-dimensional interdependent geographic objects formed within the cryolithozone according to the Milkov's theory [1]: rocks, surface and groundwater, climate, soil, and biota.

The recognition by remote sensing of these five geographic components structuring the permafrost-mountain landscape in Siberian Arctic region allows modeling the evolution of the Arctic landscape and analyses the current dynamics and interactions. The spatio-temporal monitoring of the five landscape geographic components gives the capacities to follow the complex dynamics of the landscape structures due to the self-transformations and the climatic variability. Furthermore, the spatial modeling gives some elements (mapping) of prediction of the degradation of the landscape potentially having impact on the infrastructure, rural centers, agricultural land, and expected (potential) opening gold and silver mines. Remote sensing is the only one available approach to analyze these landscape processes

in this region because of the inaccessibility of the area. Remote sensing is also used to analyze the heterogeneity of mountain permafrost landscapes: classifications generated are more accurate and detailed and they are related to the Milkov's taxonomy. Many studies have evaluated the feasibility of mapping permafrost landscapes using remote sensing [2], [3], [4]. However, most of these studies focus on the validation and on the joint interpretation of field observations and measurements. The aim of this study is to provide an original approach to the classification and mapping of permafrost mountain landscapes based on multi-fusion of image classifications (series of intra-seasonal land cover, landform classification and land surface temperature) using existing taxonomical basis [5], [6], [7] for interpreting landscape components.

## 2. MATERIALS AND METHODS

### 2.1. Arctic mountain permafrost landscapes

The study area has a size of 60x100 km and lies between latitude 68°24,1'– 67°34,3' N and longitude 129°14,5' – 131°32' E. It is the Orulgan ridge, the North-eastern part of the Verkhoyansk Mountain ridge system in Siberia. According to the permafrost landscape map [8], this Arctic region is composed of mountain deserts, mountain tundra and sparse forests, as well as intrazonal valley landscapes: north-taiga and mountain taiga, and mountain tundra.

The vegetation repartition combines different types and associations [9]. It is used for the mapping of land cover and vegetation classification.

### 2.2. Remote sensing and DEM data

Sentinel 2A images (4 bands: 490nm, 560nm, 665nm and 842nm at 10m spatial resolution) were used in this research. They were obtained during the summer vegetative period for the recognition and classification of vegetation with Support Vector Machine classifier. Sentinel 2A images were acquired on the 15<sup>th</sup> of June 2019, 12<sup>th</sup> of July 2019 and 29<sup>th</sup> of August 2019. Landform classification using Jenness's algorithm from ASTER data was processed from 6 scenes of ASTER GDEM. Landsat 8 OLI/TIRS was acquired on the 28<sup>th</sup> of August 2018 for recognizing the permafrost categories

(types) by the Land surface temperature modeling. Preprocessing for Sentinel 2A and Landsat 8 OLI/TIRS data includes radiometric calibration and atmospheric correction applied DOS 1.

## 2.2. Multi-fusion modeling approach

The multi-fusion data modeling approach (Fig. 1) includes three methods for landscape object recognition: land cover (Section 2.2.1) and landform (Section 2.2.2) classification [10], and land surface temperature (Section 2.2.3).

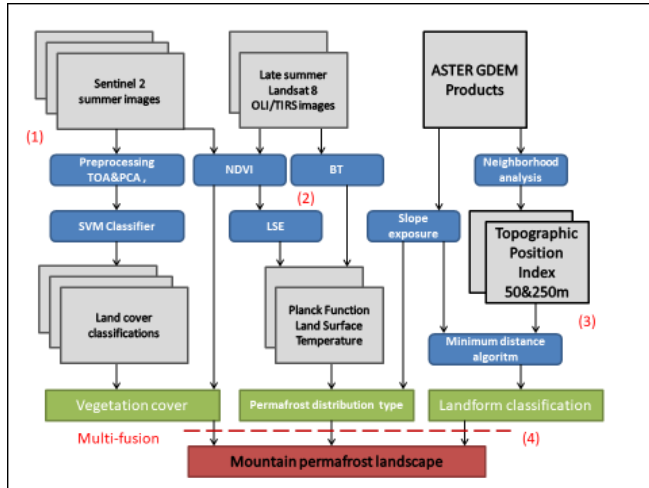


Fig. 1. Mountain permafrost landscape multi-fusion modeling

### 2.2.1. Land cover classification

The method of land cover analysis has three main steps:

- 1) The image enhancement that is performed by principal component analysis (PCA) to reduce dimensionality to the 4 spectral bands: three principal components contain 91% of spectral (radiometric) information of 4 bands of Sentinel 2A.
- 2) Supervised spectral classification by the Support Vector Machine (SVM) algorithm [11], [12] using the radial basis function (RBF) of the kernel type and C-Support model: we selected 23 training geographic object areas on Sentinel 2A acquired in June, July and August vegetative period. These training areas correspond with the land cover classes (forest, rare forest, bushes, shrubs, grass, moss, bare soil, and water).
- 3) Calculation of the overall accuracy of land cover classifications by the error matrix and the kappa coefficient respectively for June (84,2% and 0.74), July (79,1% and 0.71) and August (81,5 % and 0.72).

The spectral classification for each summer dates gives a good result according to the differences of brightness characteristics of vegetation species during the observation period [13].

### 2.2.2. Landform classification by ASTER GDEM

Compilation of ASTER GDEM data scenes (30m resolution) generates the mesorelief types obtained by the automatic landform classification using Jenness algorithm [14] based on Topographic Position Index (TPI). The TPI algorithm compares the values of each cell inside the DEM with the average of a specific neighborhood around the cell. Landform classification made using TPI is performed with 5x5 window neighborhood analysis at 250m (Fig.2 a) and at 500m (Fig. 2 b) radius (small and large scales) (Fig. 2, a, b) calculating slope degrees and altitudes. Five types of landform related to mesorelief characteristics are recognized (Table 1).

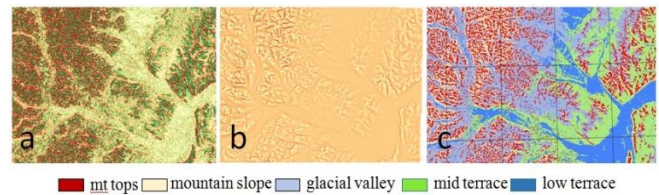


Fig. 2. a) TPI 250 m; b) TPI 500 m; c) landform classification Table 1. Landform Classification modified according to mesorelief characteristics:

Landform types	Samples
Mountain tops	Small Neighborhood TPI $\geq 1$ ; Large Neighborhood TPI $\geq 1$ ; Slope $\leq 5^\circ$
Mountain slope	Small Neighborhood $-1 < \text{TPI} < 1$ ; Large Neighborhood TPI $\geq 1$ ; Slope $\geq 5^\circ$
Glacial valley	Small Neighborhood $-1 < \text{TPI} < 1$ Large Neighborhood TPI $\leq -1$
Mid-terrace	Small Neighborhood TPI $\leq -1$ ; Large Neighborhood TPI $\geq 1$
Low-terrace	Small Neighborhood: $-1 < \text{TPI} < 1$ Large Neighborhood: $-1 < \text{TPI} < 1$ Slope $\leq 15^\circ$ Height $\leq 500$

We used altitude (height) to distinguish mid and low terraces for the river valley landform object with similar TPI and slope characteristics.

### 2.2.3. Land Surface Temperature (LST)

LST was determined by thermal infrared image from Landsat 8 TIRS sensor. LST is estimated by Planck Function (1) [15] using Brightness Temperature algorithm (BT). The Land Surface Emissivity (LSE) is calculated by the logarithmic relationship of the NDVI made by Landsat 8 OLI sensor with bands 4 (red) and 5 (NIR) with the surface emissivity.

$$LST = BT / \{1 + [\lambda \cdot BT / \rho] \cdot \ln LSE\} \quad (1)$$

$\lambda$  is the central band wavelength of emitted radiance (1080 nm for band 10;  $\rho$  is  $h \times c / \sigma$  ( $1.438 \times 10^{-2}$  m K), with  $\sigma$  as the Boltzmann constant ( $1.38 \times 10^{-23}$  J/K),  $h$  - Planck's constant ( $6.626 \times 10^{-34}$  J\*s), and  $c$  as the velocity of light ( $2.998 \times 10^8$  m/s). The calculated LST value is then converted to Celsius degree. The late summer images allow to analyze

surfaces with a seasonally thawed layer of permafrost including the weak effect of vegetation activity.

### 3. MOUNTAIN PERMAFROST LANDSCAPE RECOGNITION

#### 3.1. Identification of landscape vegetation association

The vegetation association (VA) and the mesorelief are the factors differentiating the landscape's types in accordance with the Milkov's theory. The combination by arithmetic fusion of summer land cover and landform classes generates the landscape VA permafrost map (Fig. 3).

$$VA = 1000 * x_1 + 100x_2 + 10 * x_3 + x_4 \quad (2)$$

The identification of VA was provided by the multi-fusion analysis of photosynthetic activities variations of land cover in different types of landform (2):  $x_1$ - landform types, land cover class -  $x_2$  (June),  $x_3$ (July),  $x_4$ (August).

Table 2. NDVI photosynthetic activities of vegetation associations

Vegetation associations (VA)	NDVI threshold			Landform object
	june	july	august	
larch forest, birch, bilberry	0,62-0,7	0,33-0,45	0,3-0,4	Mid terrace
larch forest lingonberry-ledum	0,57-0,62	0,45-0,5	0,25-0,33	
subalpine-shrubby	0,43-0,57	0,33-0,45	0,3-0,4	Glacial valley
mixed grass meadows	0,57-0,34	0,6-0,75	0,25-0,35	
wet meadow	0,43-0,5	0,40-0,52	0,3-0,35	
willow shrubs	0,23-0,5	0,3-0,45	0,3-0,35	Mountain slope
larch forest moss	0,34-0,65	0,5-0,55	0,34-0,45	
tussock meadow	0,15-0,2	0,15-0,25	0,12-0,2	
subalpine-lichen with juniper thickets	0,15-0,3	0,05-0,3	0,05-0,3	
alpine meadow	0,1-0,2	0,14-0,25	0,1-0,2	Mountain tops
dryads alpine	0,67-0,72	0,6-0,75	0,6-0,74	
epilithic-lichen	0,05-0,15	0,05-0,2	0,05-0,2	
larch forest low-terraced	0,67-0,72	0,5-0,65	0,5-0,56	Low terrace
valley mixed forests	0,6-0,67	0,6-0,75	0,35-0,55	
willow shrub low-terraced	0,43-0,46	0,46-0,55	0,2-0,45	

The photosynthetic activities of the vegetation land cover classes were calculated by NDVI. We have found that in the mountain arctic sparse forest, the vegetation index reflects not only the upper stage of vegetation, but also the lower vegetation stages (shrub, grass, moss). The table 2 presents NDVI threshold variation of identified vegetation association. Fifteen VA were extracted from the 2566

combinations of raster values by reclassification (assignment of a new class code of the obtained VA value in accordance with the identification affiliation to the type of vegetation association [16], [17].

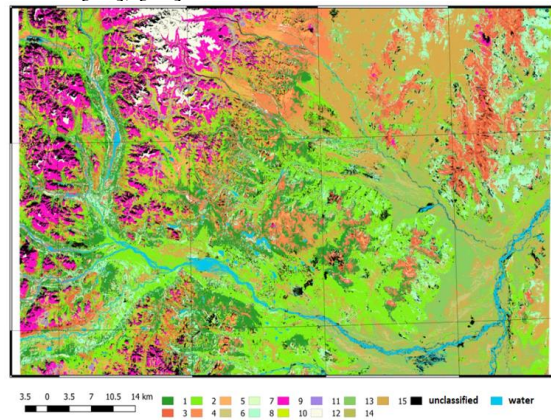


Fig. 3. Vegetation association map. 1) larch forest, birch bilberry, 3) larch forest, lingonberry-ledum, 2) cubalpine-shrubby, 4) mixed grass meadow, 5) wet meadows, 6) willow shrubs, 7) larch forest moss, 8) tussock meadow, 9) subalpine-lichen with juniper thickets, 10) alpine meadow, 11) dryads alpine, 12) epilithic-lichen, 13) larch forest low-terraced, 14) valley mixed forest, 15) willow shrub low terraced

#### 3.2. Permafrost characteristics categories

The permafrost characteristics are modelled in GIS by the thermal surfaces, slopes and exposures. The frozen surfaces are modelled by the following factors: the lower brightness temperatures, the higher emissivity, and the greater optical thickness [18]. The lack of data on snow cover did not allow us to determine frozen and unfrozen lands.



Fig. 4. Permafrost distribution map transition (green), continuous (yellow), permafrost in stone field (grey) and water (blue)

Moreover, this model based on the above indicators allows to identify transitionally frozen surface characteristics of the warm slopes of mountains not covered by woody vegetation and frozen surface of stone fields of high mountains. Three categories of permafrost characteristics are result of calculus by maximum similarity of the LST, slope degree, northern and southern exposures by the supervised classification

algorithm of the minimum Euclidean distance with 17 training areas (Fig. 4). These categories enable to differentiate between the types of frozen and thawed soils and to characterize the frozen state of the landscape.

#### 4. CONCLUSION

Synergistic use of remote sensing image processing and GIS modeling creates unprecedented opportunities for the mapping and accurate observation of changes of mountain permafrost landscape of Verkhoyansk region. This article presents an application of the Milkov's theory based on remote sensing to the characterization and categorization of the mountain permafrost landscapes. The methodology developed is based on the multi-fusion data modeling of the summertime vegetation association mapping by Sentinel 2A visible and near infrared bands with landform types generated by ASTER GDEM. The model identifies 15 vegetation associations. The implementation of the LST obtained from the Landsat 8 TIRS sensor calculus according to the brightness temperature and the land surface emissivity creates acceptable results for the modeling permafrost characteristics in Arctic mountainous territories.

#### 5. ACKNOWLEDGMENTS

This research was supported by the French National Research Agency (ANR) through the PUR project (ANR-14-CE22-0015), the North Eastern Federal University, and the Vernadski Grant of the French Embassy in the Russian Federation.

#### 6. REFERENCES

[1] Milkov F. N. The landscape sphere of the Earth., Mysl, Moscow, 1970.

[2] J. Boike, T. Grau, B. Heim, F. Gunther F., M. Langer, S. Muster, I. Gouttevin, and S. Lange. Satellite-derived changes in the permafrost landscape of central Yakutia, 2000–2011: Wetting, drying, and fires, *Global and Planetary Change*, vol. 139, pp. 116-127.

[3] Fedorov A.N. Permafrost landscapes of Yakutia: methods of isolation and mapping issues, Institute of permafrost SB RAS, Yakutsk, 140 p., 1991.

[4] S.V. Kalinicheva, M.N. Zheleznyak, A. R. Kirillin, and A. N. Fedorov. Identification and mapping of frozen areas using satellite imagery (on the example of the Elkonsky horst in South Yakutia), *Science and Education*, n°3, pp. 30-37, 2017.

[5] P. Lemenkova, B. Forbes, and T. Kumpula. Mapping Land Cover Changes Using Landsat TM: A Case Study of Yamal Ecosystems, Arctic Russia, *XI International Conference on Geoinformatics, Theoretical and Applied Aspects*, National Academy of Sciences of Ukraine, Kiev, Ukraine, 2012.

[6] S.Y. Popov. The experience of creating a geobotanical map by discriminant analysis of field and distance data, *Sovremennye problemy distantsionnogo zondirovaniya Zemli iz kosmosa*, vol. 13, n°1, pp. 25-35, 2016.

[7] I.A. Lavrinenko. Using remote sensing methods for geobotanical zoning of East European tundra, *Sovremennye problemy distantsionnogo zondirovaniya Zemli iz kosmosa*, vol. 9, n°3, pp. 269-276, 2012.

[8] A.N. Fedorov, et al. Permafrost-Landscape Map of the Republic of Sakha (Yakutia) on a Scale 1:1 500 000, *Geosciences*, vol. 8, n°465, 2018.

[9] Nikolin E.G. Flora of the Verkhoyansk Range and its spatial organization, *PhD Memory of Biology Sciences*, North Eastern Federal University, Yakutsk, 2012.

[10] M. Zakharov, S. Gadal, and Y. Danilov. Permafrost landscape categorization based on land cover, digital elevation model, land surface temperature on Verkhoyansk Mountain Ridge, *3rd International Land Use Symposium*, Paris, 2019.

[11] M. Pal, and P. M. Mather. Support vector machines for classification in remote sensing, *International Journal of Remote Sensing*, vol. 26, n°5, pp.1007-1011, 2005.

[12] M. Weinmann, and U. Weidner. Land-Cover and Land-Use Classification Based on Multitemporal Sentinel-2 Data, *International Geoscience and Remote Sensing Symposium 2018*, Valencia, Spain, 2018.

[13] Stytsenko E.A. Development of a technique for automated interpretation of a vegetation cover with the integrated use of multi-season zonal space images, *PhD Memory of Engineering Sciences*, North Eastern Federal University, Yakutsk, 2018.

[14] M. Mokarram, G. Roshan, and S. Negahban. Landform classification using topography position index (case study: salt dome of Korsia-Darab plain, Iran). *Modeling Earth Systems and Environment*, n°40, 2015.

[15] I. Ndossi, and U. Avdan. Application of Open Source Coding Technologies in the Production of Land Surface Temperature (LST) Maps from Landsat: A PyQGIS Plugin, *Remote Sensing*, vol. 8, n°413, 2016.

[16] A. Alkhatlan, A. Bannari, T.S. Ali, A. Abahussain, and N. Hameid. Mapping submerged aquatic vegetation in shallow water of Arabian gulf using water spectral indices, field observations and Landsat-OLI data. *IEEE Transactions on Geoscience and Remote Sensing*, vol. 48, n°1, pp. 511-522, 2010.

[17] S. Gadal, and W. Ouerghemmi. Knowledge Models and Image Processing Analysis in Remote Sensing: Examples of Yakutsk (Russia) and Kaunas (Lithuania), *5th International Conference on Geographical Information Systems Theory, Applications and Management*, Heraklion, Greece, pp. 282-288, 2019.

[18] T. Zhang, R. G. Barry, and R. L. Armstrong. Application of satellite remote sensing techniques to frozen ground studies. *Polar Geography*, vol.28, n°3, pp.163–196, 2004.